Received: 11 November 2019 | Revised: 8 May 2020 | Accepted: 12 May 2020

DOI: 10.1002/nbm.4343

RESEARCH ARTICLE

NMR IN BIOMEDICINE WILEY

Metabolite cycled liver ^{1}H MRS on a 7 T parallel transmit system

Aline Xavier[1,2,3] | Catalina Arteaga de Castro[1] | Marcelo E. Andia[2,3] | Peter R. Luijten[1] | Dennis W. Klomp[1] | Ariane Fillmer[1,4] | Jeanine J. Prompers[1]

[1]Department of Radiology, Imaging Division, University Medical Center Utrecht, Utrecht, The Netherlands

[2]Biomedical Imaging Center, Pontificia Universidad Católica de Chile, Santiago, Chile

[3]Millennium Nucleus for Cardiovascular Magnetic Resonance, Santiago, Chile

[4]Physikalisch-Technische Bundesanstalt (PTB), Berlin, Germany

Correspondence
Jeanine J. Prompers, PhD, Department of Radiology, Imaging Division, University Medical Center Utrecht, Heidelberglaan 100, 3584 CX, Utrecht, The Netherlands.
Email: j.j.prompers@umcutrecht.nl

Funding information
CONICYT-PCHA/Doctorado Nacional, Grant/Award Number: 2016-21160835; FONDECYT, Grant/Award Number: 1180525; Millennium Science Initiative of the Ministry of Economy, Development and Tourism, Chile, Grant/Award Number: Nucleus for Cardiovascular Magnetic Resonance; Nederlandse Organisatie voor Wetenschappelijk Onderzoek (NWO), Grant/Award Number: 040.11.634

Introduction: Single-voxel ^{1}H MRS in body applications often suffers from respiratory and other motion induced phase and frequency shifts, which lead to incoherent averaging and hence to suboptimal results.

Methods: Here we show the application of metabolite cycling (MC) for liver STEAM-localized ^{1}H MRS on a 7 T parallel transmit system, using eight transmit-receive fractionated dipole antennas with 16 additional, integrated receive loops. MC-STEAM measurements were made in six healthy, lean subjects and compared with STEAM measurements using VAPOR water suppression. Measurements were performed during free breathing and during synchronized breathing, for which the subjects did breathe in between the MRS acquisitions. Both intra-session repeatability and inter-session reproducibility of liver lipid quantification with MC-STEAM and VAPOR-STEAM were determined.

Results: The preserved water signal in MC-STEAM allowed for robust phase and frequency correction of individual acquisitions before averaging, which resulted in in vivo liver spectra that were of equal quality when measurements were made with free breathing or synchronized breathing. Intra-session repeatability and inter-session reproducibility of liver lipid quantification were better for MC-STEAM than for VAPOR-STEAM. This may also be explained by the more robust phase and frequency correction of the individual MC-STEAM acquisitions as compared with the VAPOR-STEAM acquisitions, for which the low-signal-to-noise ratio lipid signals had to be used for the corrections.

Conclusion: Non-water-suppressed MC-STEAM on a 7 T system with parallel transmit is a promising approach for ^{1}H MRS applications in the body that are affected by motion, such as in the liver, and yields better repeatability and reproducibility compared with water-suppressed measurements.

Abbreviations: B_0, *main magnetic field*; B_1^+, *transmit field*; CR, coefficient of repeatability/reproducibility; CSDE, chemical shift displacement error; CV, coefficient of variation; MC, metabolite cycling/cycled; NAFLD, non-alcoholic fatty liver disease; ROI, region of interest; SD, standard deviation; SNR, signal-to-noise ratio; STEAM, stimulated echo acquisition mode; tCho, total choline; UHF, ultra-high field; UI, unsaturation index; VAPOR, variable pulse powers and optimized relaxation delays..

Ariane Fillmer and Jeanine J. Prompers shared senior authorship.

KEYWORDS
7 T, lipid composition, lipids, liver, metabolite cycling, MRS, parallel transmit, ultra-high field

1 | INTRODUCTION

Hepatic steatosis is a hallmark of non-alcoholic fatty liver disease (NAFLD), the most common liver disorder in the Western world, which can evolve into non-alcoholic steatohepatitis, liver cirrhosis, and hepatocellular carcinoma.[1,2] In addition to the highly elevated amounts of lipid in the liver, NAFLD is also associated with marked changes in liver lipid composition. In obese patients with NAFLD, hepatic saturated fatty acids are significantly increased at the expense of polyunsaturated fatty acids.[3–5]

Localized ^{1}H MRS has proven to be a reliable tool for the in vivo quantification of lipid content in the liver, showing strong correlations with liver biopsy results.[6–10] In addition, ^{1}H MRS has been applied as a non-invasive method for the analysis of liver lipid composition based on the olefinic, diallylic and allylic lipid proton signals.[6,7,11] Using these ^{1}H MR signals, Johnson et al[7] showed that the relative hepatic lipid saturation increases and polyunsaturation decreases with obesity. However, at common clinical magnetic field strengths (1.5-3.0 T), the spectral resolution of liver ^{1}H MR spectra is limited, hampering accurate determination of lipid composition.

Ultra-high field (UHF; main magnetic field (B_0) ≥ 7.0 T) MRS provides increased spectral resolution, which should improve the reliability of the assessment of liver lipid composition. However, UHF-MRS in the liver is challenging because of large B_0 and transmit field (B_1^+) inhomogeneities. UHF-MRI systems are not equipped with a ^{1}H body transmit coil and hence local transmit coils have to be used. Gajdošík et al have recently shown the application of ultrashort-T_E stimulated echo acquisition mode (STEAM) MRS for the quantification of liver lipid content and composition at 7 T using a surface coil for transmit and receive, which is associated with large B_1 inhomogeneities and limited penetration depth.[12] Recent advances in RF transmit coil array design have shown the beneficial use of fractionated dipole antennas for body imaging at UHF, providing increased transmit efficiency and homogeneity within the specific absorption rate limits.[13] Moreover, it was shown that combining dipole antennas with loop coils in receive arrays enhances the signal-to-noise ratio (SNR) compared with receiving with dipoles or loops only.[14] A setup consisting of fractionated dipole antennas combined with additional receive-only loops is therefore expected to be beneficial for liver MRS at 7 T, allowing measurements at various locations in the liver (eg anterior, lateral or posterior locations), including also less superficial parts.

An additional challenge for liver MRS is that respiratory and other physiologic and subject motion induces phase and frequency shifts, which leads to incoherent averaging and hence to suboptimal results. Metabolite cycling (MC)[15–17] has been proven beneficial, especially for small voxel volumes that are influenced by motion.[18–20] MC makes use of an inversion pulse[21] to alternately invert the signal of the metabolites upfield or downfield of water, while leaving the water magnetization untouched. The advantage of the latter is that the unsuppressed water signal can be used for phase and frequency correction of the individual acquisitions, which is more accurate than using the low-SNR metabolite signals in water-suppressed spectra. Subtraction of the upfield and downfield inverted spectra effectively cancels the water signal and, importantly, the gradient induced modulation sidebands, leaving a clean metabolite spectrum from which also low-concentration metabolites can be reliably quantified. The sum of the upfield and downfield inverted spectra, on the other hand, provides a water spectrum, which can be used as an internal reference for quantification. These benefits of MC in combination with the application of parallel transmission technology and advanced RF coils enable the acquisition of high-quality UHF ^{1}H MRS data in the liver with a greater flexibility for positioning the volume of interest.

Here we show the application of MC for liver ^{1}H MRS on a 7 T parallel transmit system, using eight transmit-receive fractionated dipole antennas with 16 additional, integrated receive loops. Because of the short T_2 relaxation times in the liver at 7 T,[12,22] localization was performed with a short-T_E STEAM sequence. The performance of MC-STEAM was compared with STEAM measurements with conventional water suppression using variable pulse powers and optimized relaxation delays (VAPOR)[23] in healthy, lean volunteers. In addition, the effect of synchronized breathing was investigated in comparison with free breathing acquisitions, and intra-session repeatability and inter-session reproducibility of liver lipid content as determined by the different acquisition methods were determined.

2 | METHODS

Data were acquired in a phantom containing a lipid emulsion (0.1 vol.% Intralipid™ soybean oil emulsion in water with 90 mM NaCl and 0.12 mM $MnCl_2$) and in the liver of six healthy, lean volunteers (age, 27-47 years; body mass index, 21.6-23.9 kg/m^2; three male, three female; Table 1). The study was approved by the local medical ethics committee and all subjects signed informed consent prior to inclusion. Each subject was scanned twice on two separate days, approximately one week apart. Conditions such as nutrition and physical activity were not standardized.

TABLE 1 Subjects' characteristics

Subject	Sex	Age (years)	BMI (kg/m^2)
1	male	37	23.0
2	male	27	23.0
3	male	44	21.6
4	female	36	22.3
5	female	28	23.9
6	female	47	23.3

BMI: body mass index.

2.1 | Data acquisition

All measurements were made on a 7 T Philips Achieva multi-transmit system (Philips Healthcare, Best, The Netherlands) with a maximal gradient amplitude of 40 mT/m at a slew rate of 200 T/m/s, using eight parallel transmit channels driven by 8 × 2 kW peak power amplifiers. Each transmit channel was connected to a transmit-receive fractionated dipole antenna[13] with two additional integrated receive-only loops (MR Coils, Zaltbommel, The Netherlands), resulting in an eight-channel transmit/24-channel receive setup.[14] The 16 receive-only loops were interfaced to a 16-channel receiver box.

First, T_1 weighted gradient echo localizer images were acquired. Then, low-flip-angle gradient echo images (2D multi-slice acquisition, T_E = 1.68 ms, T_R = 30 ms, FOV = 350 × 457 × 30 mm^3, in-plane resolution = 3.9 × 3.8 mm^2, slice thickness = 10 mm, flip angle = 3.5°) were acquired in three slices in the liver for every transmit channel, which were used for RF phase shimming.[24] Optimum phase settings to obtain maximum signal intensity in a region of interest (ROI) in the right lobe of the liver (averaged over three slices) were calculated with a numerical minimization in MATLAB (MathWorks, Natick, Massachusetts). Amplitudes of the channels were all set equal. For both the phantom and the in vivo measurements, RF phase shimming resulted in a B_1^+ of 16-19 μT in the ROI, which was quantified from a B_1 map measured using the actual flip angle imaging method[25] (3D gradient echo, T_E = 2.3 ms, T_R = 50 and 250 ms, FOV = 280 × 420 × 30 mm^3, resolution = 3.9 × 3.8 × 10 mm^3, flip angle = 55°). A 3D B_0 map (3D gradient echo, T_E = 1.49 ms, ΔT_E = 1.0 ms, T_R = 10 ms, FOV = 280 × 402 × 78 mm^3, resolution = 4.4 × 6.0 × 6.0 mm^3, flip angle = 5°) was acquired during a breath hold in the exhaled state (acquisition time = 16.3 s) for B_0 shimming. Linear and second order shim settings were optimized over the ROI in the right lobe of the liver, while a region of less interest covering the whole liver was also considered during the calculation, albeit with a lower weight,[26] using the MR Code software (MR Code, Zaltbommel, The Netherlands). A Dixon[27] scan (2D multi-slice gradient echo, T_E = 2.6 ms, ΔT_E = 0.5 ms, T_R = 10 ms, FOV = 282 × 360 × 80 mm^3, in-plane resolution = 1.3 × 1.3 mm^2, slice thickness = 4 mm, 20 slices, flip angle = 15°) was performed after RF phase and B_0 shimming, which was used for planning of the MRS voxel.

STEAM spectra were acquired in a 15 × 15 × 20 mm^3 voxel positioned in the right lobe of the liver, in the same region where B_1 and B_0 fields were optimized. Major vessels and biliary structures (more concentrated in the deeper lying regions of the liver) and edges of the liver were avoided, while taking care that voxels for both the water and lipid methylene frequencies were surrounded by homogeneous liver tissue. Spectra were acquired with water suppression using VAPOR (100 Hz bandwidth for the phantom and 200 Hz bandwidth for the in vivo liver measurements), including a water reference scan, and without water suppression using MC. For the latter, the STEAM sequence was modified to include an asymmetric adiabatic MC inversion pulse[21] in the mixing period[15,19] (MC pulse duration = 22.4 ms). The offsets for the MC pulses were +175 Hz and −175 Hz from the water frequency for odd and even scans, respectively. In the phantom, also a MC-STEAM spectrum was recorded with MC pulse offsets of +50 Hz and −50 Hz, for a more fair comparison with the VAPOR-STEAM spectrum with a 100 Hz bandwidth for the VAPOR water suppression. Other scan parameters for the MRS measurements were as follows: spectral bandwidth = 4000 Hz, data points = 1024, T_E = 10 ms, T_M = 38 ms, T_R = 2500 ms, N_{avg} = 64/128 (phantom/liver). For the in vivo measurements, in each session both VAPOR-STEAM and MC-STEAM spectra were acquired once with free breathing and twice with synchronized breathing, resulting in six MRS measurements per session. For the measurements with synchronized breathing, the volunteers were instructed to synchronize their breathing with the sound of the applied sequence, such that acquisitions were performed in the exhaled state. The repeated measurements with synchronized breathing within each session (both for VAPOR-STEAM and MC-STEAM) were used to determine the intra-session repeatability of the quantification of liver lipid content. For each subject, the whole scan protocol was repeated on two different days, approximately one week apart, to determine the inter-session reproducibility. Care was taken to keep the positioning of the MRS voxel, which was guided by anatomical landmarks, as constant as possible between sessions.

2.2 | MRS data processing and quantification

The signals of the individual acquisitions (one per T_R) of the 24 channels (eight transmit-receive fractionated dipole antennas and 16 receive loops) were individually phased and eddy current corrected before channel combination, frequency alignment and averaging, using an in-house written

MATLAB script. Eddy current correction of the VAPOR-STEAM data was performed using the water reference scan. Channel combination was performed using the generalized least squares (GLS) algorithm,[28,29] using all averages for the MC-STEAM scans or only the water reference scan for the VAPOR-STEAM measurements to estimate the coil sensitivities. After channel combination, frequency alignment was performed based on frequency domain correlation.[30] For the MC-STEAM spectra, correlations were calculated for the spectral region containing the water peak, while for the VAPOR-STEAM spectra the spectral region to calculate the correlations included the lipid methyl signal (0.90 ppm) up to the signal from choline containing compounds (3.22 ppm). For the MC-STEAM spectra, signals were separately averaged for the odd and even acquisitions, which were then summed and subtracted to yield the water and metabolite signals, respectively.

Spectra were fitted with the advanced method for accurate, robust and efficient spectral fitting (AMARES) in the jMRUI software package[31,32] without any further post-processing, such as apodization or removal of the residual water signal from the metabolite spectra. In the water spectra, the water signal was fitted by a single Lorentzian line. In the metabolite spectra, the lipid resonances at 5.30 (olefinic methine, -C***H***=C***H***-), 2.77 (diallylic methylene, -CH=CH-C***H***$_2$-CH=CH-), 2.24 (α-carboxylic methylene, -C$_α$***H***$_2$-COO-), 2.02 (allylic methylene, -C***H***$_2$-CH=CH-C***H***$_2$-), 1.62 (β-carboxylic methylene, -C$_β$***H***$_2$-CH$_2$-COO-), 1.30 (methylene, (-C***H***$_2$-)$_n$) and 0.90 (methyl, -C***H***$_3$) ppm and the signal from choline containing compounds (total choline, tCho) at 3.22 ppm were fitted by Lorentzian lines with equal linewidths. To make the fitting more robust, amplitudes of the α-carboxylic methylene, β-carboxylic methylene and methyl peaks at 2.24, 1.62 and 0.90 ppm were constrained to have ratios of 1:1:1.33, as theoretically predicted from the number of protons and the T_1 and T_2 relaxation time constants.[22] For the MC-STEAM spectra, fitting of the olefinic methine peak at 5.3 ppm was omitted.

Liver lipid content was calculated as $L/(L + W) \times 100\%$, where W represents the amplitude of the water signal (in the time domain, corresponding to the integral in the frequency domain) and L the total amplitude of the following lipid signals: diallylic methylene, α-carboxylic methylene, allylic methylene, β-carboxylic methylene, methylene and methyl (2.77, 2.24, 2.02, 1.62, 1.30 and 0.90 ppm). Signals were corrected for T_1 and T_2 relaxation using the relaxation time constants as determined by Gajdošík et al.[22] The unsaturation index (UI) was calculated according to Johnson et al[7] as the ratio of the sum of the amplitudes of the diallylic and allylic methylene signals (2.77 and 2.02 ppm) to the sum of the amplitudes of the diallylic methylene, allylic methylene, methylene and methyl signals (2.77, 2.02, 1.30 and 0.90 ppm), corrected for T_1 and T_2 relaxation.

2.3 | Statistical analysis

Data are presented as means ± standard deviation (SD). Statistical significance of differences in SNR and linewidth between reconstruction without and with frequency correction, measurements with free and synchronized breathing (using the first synchronized scans) and measurements with VAPOR-STEAM and MC-STEAM were assessed by applying a three-way analysis of variance for repeated measures, followed by Bonferroni corrected post-hoc tests using the IBM SPSS 25.0 statistical package (SPSS, Chicago, Illinois). Differences in liver lipid content between repeated measurements within one session and repeated measurements between two sessions were assessed using paired samples t-tests. Statistical significance was set at $p < 0.05$.

Comparisons of liver lipid content measured with free and synchronized breathing and with VAPOR-STEAM and MC-STEAM were made using Bland-Altman analyses. Intra-session and inter-session variability of liver lipid content and intra-session variability of UI were also assessed using Bland-Altman analyses. Coefficients of repeatability/reproducibility (CRs) were calculated from the SD of the signed differences between two scans for each subject according to $CR = 1.96 \times SD$. Coefficients of variation (CVs) were calculated as the SD of the differences divided by the mean. Correlation between UI and liver lipid content was assessed using Pearson's correlation.

3 | RESULTS

3.1 | Phantom measurements

Figure 1A-C compares VAPOR-STEAM and MC-STEAM spectra recorded on the phantom with a lipid emulsion. Using MC-STEAM, the subtraction of downfield and upfield inverted spectra led to a spectrum free of sidebands, with good water cancellation. However, the olefinic lipid signal, which is close to the water peak (5.3 ppm), could not clearly be observed in the MC-STEAM spectrum with MC pulse offsets of +175 Hz and −175 Hz (Figure 1B), which were also used for the in vivo measurements, whereas the (inverted) peak is clearly resolved in the MC-STEAM spectrum with MC pulse offsets of +50 Hz and −50 Hz (Figure 1C). The signal intensities of the other lipid resonances were comparable for VAPOR-STEAM and MC-STEAM. By varying the power for the asymmetric adiabatic MC inversion pulse, it was shown that a B_1^+ above 15 μT in the ROI is required for complete inversion of the lipid methylene signal at 1.30 ppm and thus to obtain the full signal amplitude in the difference spectra (Figure 1D). This condition was met for all in vivo measurements.

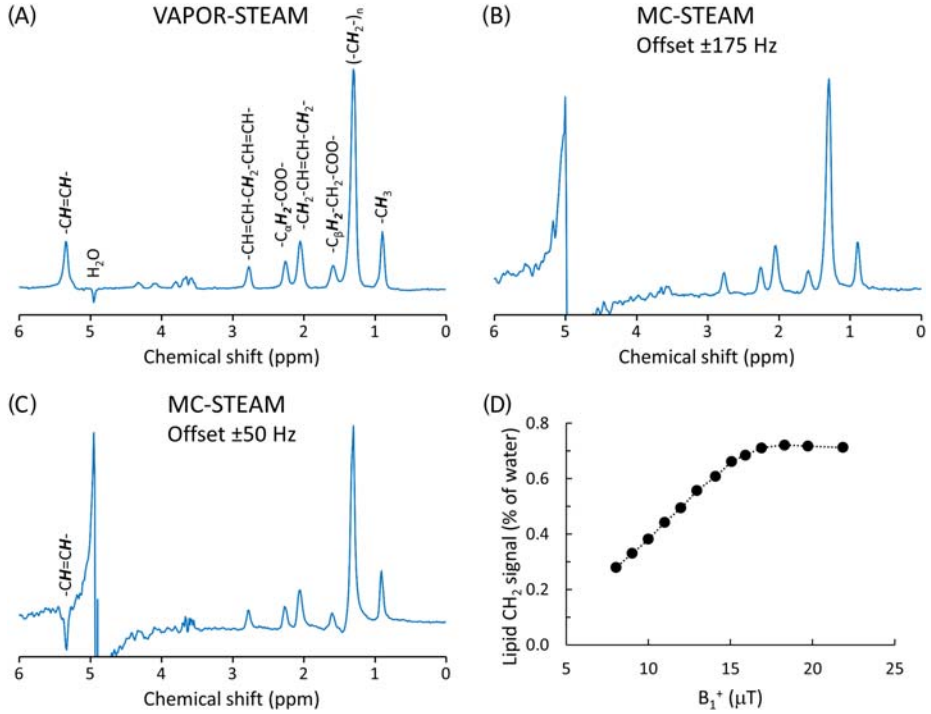

FIGURE 1 A-C, Spectra acquired in a phantom containing a lipid emulsion using a conventional STEAM sequence and VAPOR water suppression (A), and MC-STEAM without water suppression (B, C). In B the offsets for the MC pulses were +175 Hz and −175 Hz from the water frequency for odd and even scans, respectively (in vivo settings), while in C the offsets for the MC pulses were +50 Hz and −50 Hz from the water frequency. All major lipid peaks in the upfield spectrum can be clearly identified within all spectra and are indicated in A. The olefinic lipid signal at 5.3 ppm, however, can only be distinguished clearly in the VAPOR-STEAM spectrum (A) and in the MC-STEAM spectrum with the smaller offsets (C; olefinic lipid signal has a 180° phase difference with the upfield signals). D, Lipid methylene signal amplitude (expressed as a percentage of the water signal) as a function of the B_1^+ used for the MC pulses. A B_1^+ above 15 μT in the ROI is required for complete inversion of the methylene signal and thus to obtain the full signal amplitude in the difference spectra

3.2 | In vivo measurements

Figure 2 shows an example of the voxel positioning for the in vivo liver measurements (see Figure S1 of the supporting material for voxel planning in all six subjects), as well as the results for the MC-STEAM acquisition. In Figure 2B the downfield and upfield inverted spectra (after individual phase correction, coil combination, frequency alignment and averaging) are separately displayed, showing an excellent efficiency of the MC inversion pulse. The sum of the downfield and upfield inverted spectra (Figure 2C) shows a clean water spectrum, whereas the difference of the downfield and upfield inverted spectra (Figure 2D) represents the metabolite spectrum.

Figure 3 compares VAPOR-STEAM and MC-STEAM spectra acquired in vivo in the liver from the voxel indicated in Figure 2A, during both free breathing and synchronized breathing and reconstructed without and with frequency correction. The positive effect of both synchronized breathing and frequency correction on lineshape and linewidth can be clearly observed in the data sets of this volunteer. Figure 4 shows the same type of data for a different subject, with a 2.3-fold lower liver lipid content as compared with the subject in Figure 3 (1.0% versus 2.3%). In this case, it is evident that frequency correction no longer leads to an improvement of the VAPOR-STEAM spectra, and in fact leads to worse lineshapes, while for the MC-STEAM spectra frequency alignment still leads to a significant enhancement of the spectral quality. For the subjects with a liver lipid content below 2%, frequency correction of the VAPOR-STEAM spectra did not give optimal results in 54% of the cases, while the effect of frequency alignment of the water signal in the MC-STEAM spectra on the metabolite difference spectra was satisfactory in all cases.

Figure 5 shows the quantification of the SNR of the lipid methylene peak (1.30 ppm) and the linewidth of the lipid peaks for all six subjects for both scan sessions. Frequency alignment did significantly improve the SNR for the data with free breathing, but not for synchronized breathing (Figure 5A). SNR was not significantly different between the spectra measured with free and synchronized breathing or between the spectra acquired with VAPOR-STEAM and MC-STEAM. Linewidths became significantly smaller when frequency alignment was applied before averaging the individual acquisitions (Figure 5B), for both the VAPOR-STEAM and the MC-STEAM scans and for both free breathing and synchronized breathing, although the effect was smaller for synchronized breathing. Linewidths also significantly improved with synchronized breathing as

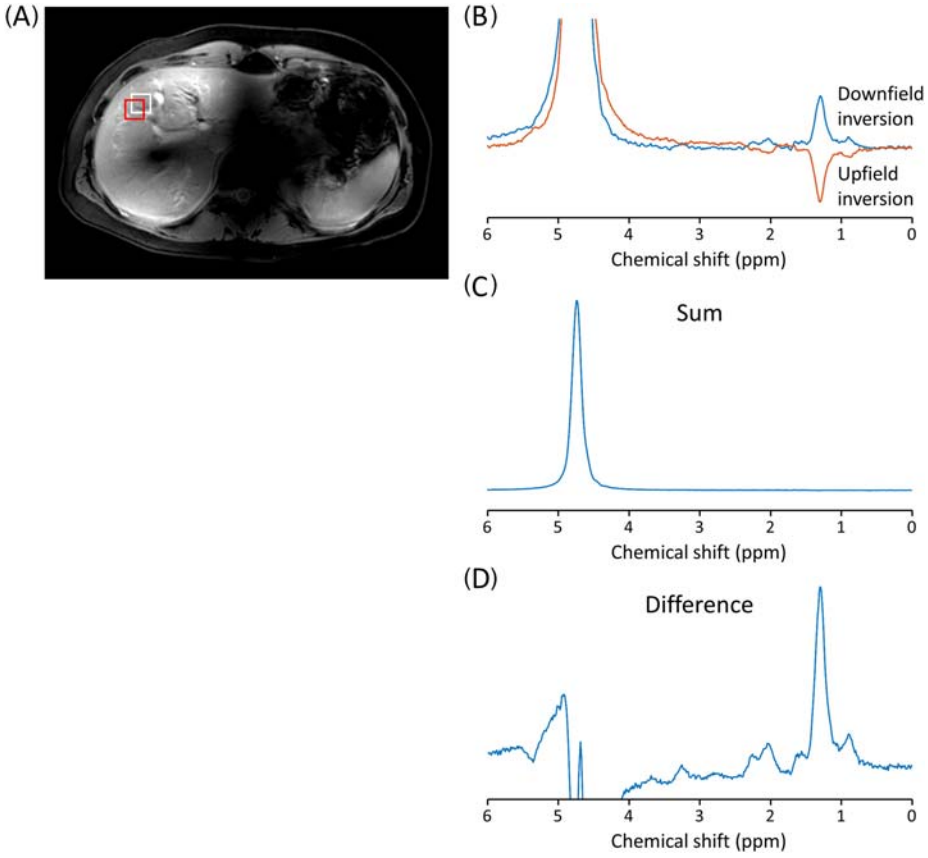

FIGURE 2 A, Example of voxel ($15 \times 15 \times 20$ mm^3) positioning in the liver depicted on a transversal Dixon scan. The red voxel indicates the voxel positioning for the water frequency, while the white voxel indicates the shifted voxel for the lipid methylene frequency. B-D, in vivo liver spectra from the voxel indicated in A using MC-STEAM: B, the downfield (blue) and upfield (red) inverted spectra (after individual phase correction, coil combination, frequency alignment and averaging); C, the sum of the downfield and upfield inverted spectra (water spectrum); D, the difference (metabolite) spectrum

compared with free breathing, for both VAPOR-STEAM and MC-STEAM and both without and with frequency correction. However, with frequency alignment, the effect of synchronized breathing on the linewidths was less pronounced.

For the remainder of the results, we only consider the data that were reconstructed with frequency correction. Figure 6 shows Bland-Altman analyses for comparisons of liver lipid content between scans with free breathing and synchronized breathing acquired with VAPOR-STEAM (A) and MC-STEAM (B) and for comparisons between scans of VAPOR-STEAM and MC-STEAM obtained with free breathing (C) and synchronized breathing (D). The difference between free breathing and synchronized breathing acquisitions was smaller for MC-STEAM than for VAPOR-STEAM (CV = 8.3% versus 14.1%), but for both acquisition methods there were no significant differences in liver lipid content between free and synchronized breathing. The CV between VAPOR-STEAM and MC-STEAM was 14.4% for free breathing acquisitions and 20.0% for synchronized breathing acquisitions. Differences in lipid content between VAPOR-STEAM and MC-STEAM were not significant for either free or synchronized breathing.

3.3 | Intra-session repeatability

For the acquisitions with synchronized breathing, the intra-session repeatability of the quantification of liver lipid content was determined during both sessions (Figure 7). Intra-session variability was smaller for MC-STEAM (CV = 9.6%) than for VAPOR-STEAM (CV = 12.2%). Furthermore, for MC-STEAM there was no bias from zero, while for VAPOR-STEAM there was a small bias (absolute bias = 0.06%). For both methods, there were no significant differences in liver lipid content between repeated measurements in the same subject.

3.4 | Inter-session reproducibility

In addition, the inter-session reproducibility of liver lipid content quantification was determined for both free breathing and synchronized breathing conditions (Figure 8). Inter-session variability was smaller for MC-STEAM (CV = 23.2% and 29.4% for free and synchronized breathing, respectively) than for VAPOR-STEAM (CV = 37.1% and 39.5% for free and synchronized breathing, respectively) and was comparable for the scans with free and synchronized breathing. For both methods, there were no significant differences in liver lipid content between repeated measurements in the same subjects.

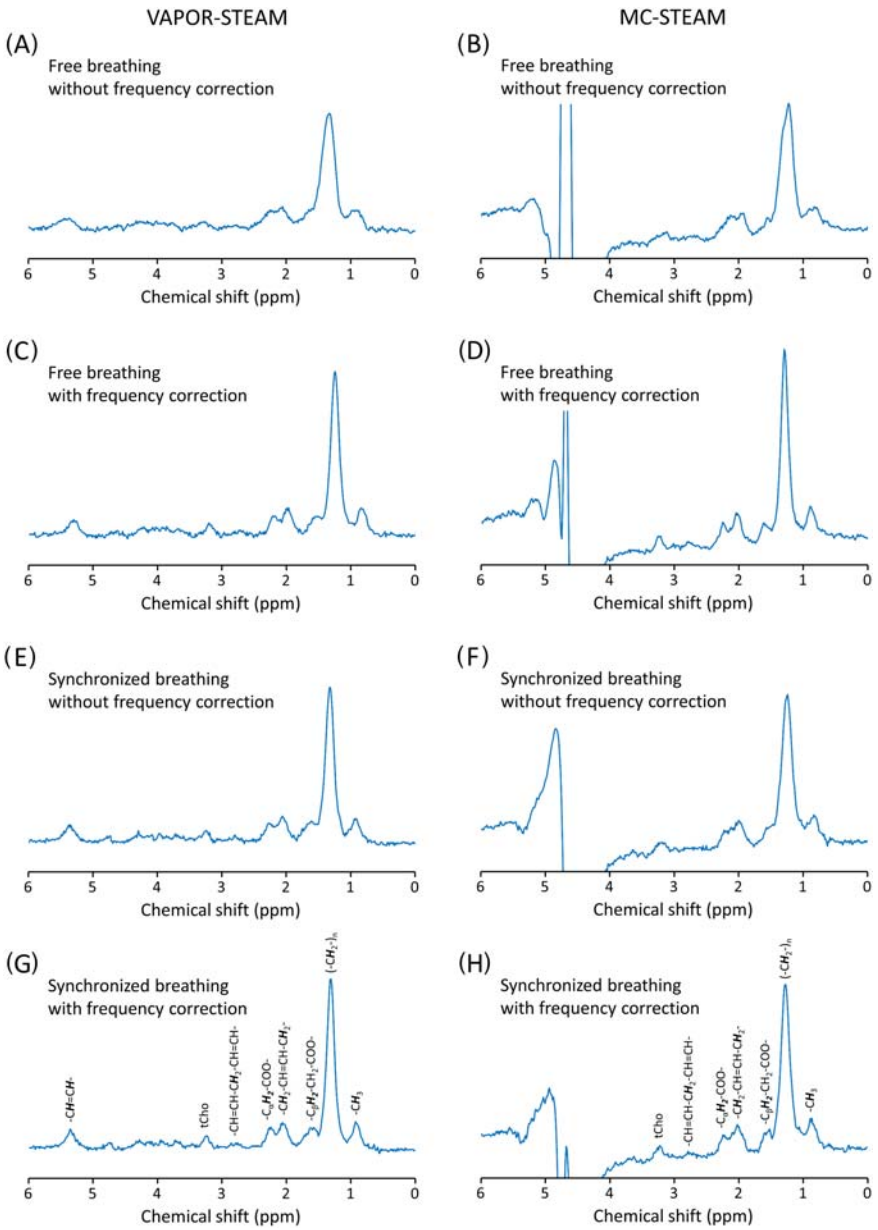

FIGURE 3 Comparison of in vivo liver spectra from the voxel indicated in Figure 2A (all in the same subject) recorded using VAPOR-STEAM (left column) and MC-STEAM (right column) with free breathing reconstructed without frequency correction (A, B) and with frequency correction (C, D), and with synchronized breathing reconstructed without frequency correction (E, F) and with frequency correction (G, H). Peak assignments are indicated in G and H. The peak at 3.22 ppm (not present in the phantom spectra) originates from tCho. Liver lipid content for this subject averaged over the different spectra was 2.3%

3.5 | Lipid unsaturation

For the acquisitions with synchronized breathing, the intra-session repeatability of the quantification of the UI of hepatic lipids was determined during both sessions (Figure 9A, B). Intra-session variability was smaller for MC-STEAM (CV = 17.2%) than for VAPOR-STEAM (CV = 51.7%). Figure 9 also shows the relation between UI and the liver lipid content, as measured with VAPOR-STEAM and MC-STEAM with synchronized breathing (Figure 9C, D). For MC-STEAM, there was a negative linear correlation between UI and lipid content ($R = -0.69$, $p = 0.01$), whereas for VAPOR-STEAM UI and lipid content were not significantly correlated ($p = 0.24$).

4 | DISCUSSION

In this study, the successful implementation of MC-STEAM for liver ^{1}H MRS on a 7 T parallel transmit system, using eight transmit-receive fractionated dipole antennas with 16 additional, integrated receive loops was demonstrated, and the performance was compared with that of STEAM measurements using VAPOR water suppression. After phase and frequency correction of the individual acquisitions (before averaging), spectra acquired with free breathing were of similar quality to spectra from measurements during which the subjects synchronized their breathing with the acquisitions. Intra-session repeatability and inter-session reproducibility of liver lipid quantification were better for MC-STEAM than for

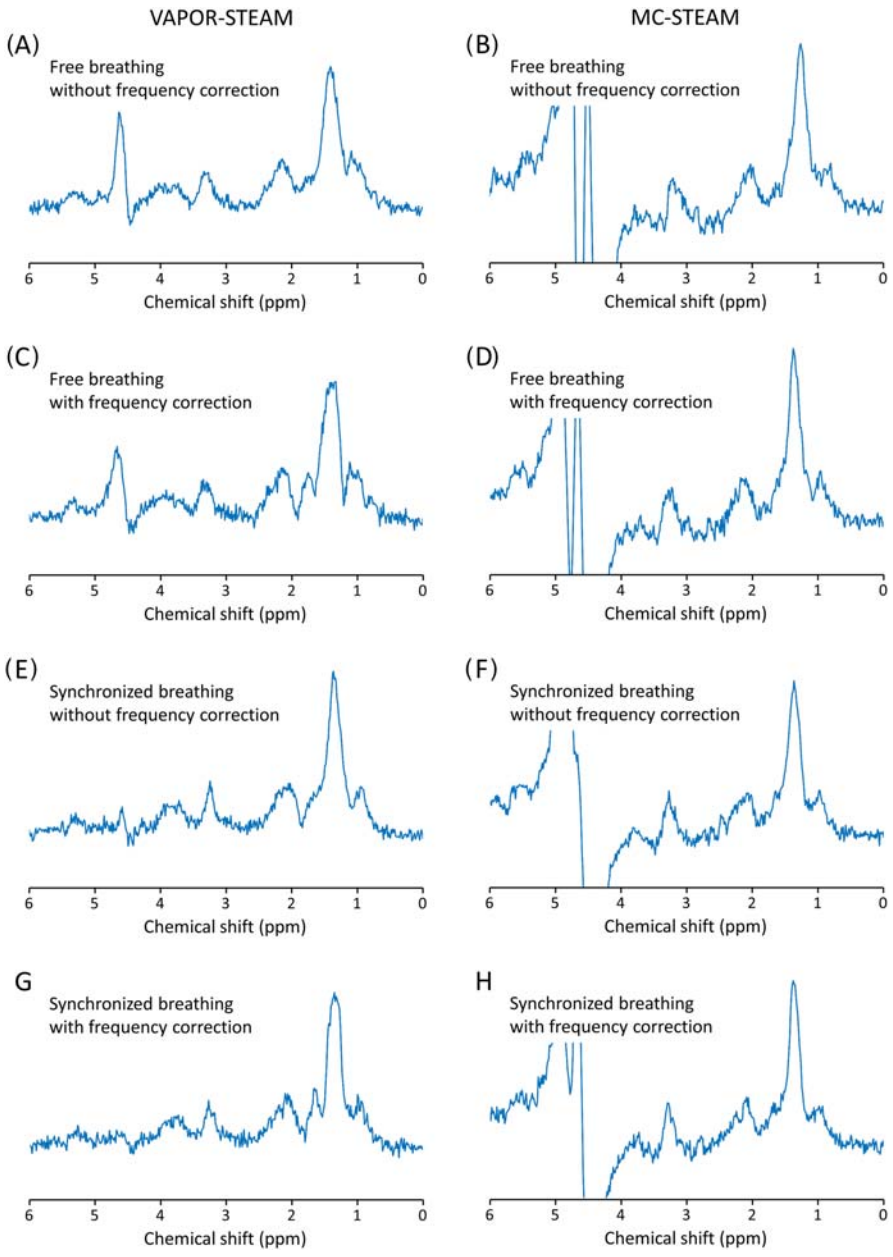

FIGURE 4 Comparison of in vivo liver spectra from another subject, with a lower liver lipid content as compared with the subject in Figure 3, recorded using VAPOR-STEAM (left column) and MC-STEAM (right column) with free breathing reconstructed without frequency correction (A, B) and with frequency correction (C, D), and with synchronized breathing reconstructed without frequency correction (E, F) and with frequency correction (G, H). Liver lipid content for this subject averaged over the different spectra was 1.0%

VAPOR-STEAM. These effects may be explained by the more robust phase and frequency correction of the individual MC-STEAM acquisitions as compared with the VAPOR-STEAM acquisitions, for which the low-SNR lipid signals had to be used for these corrections.

To date, at 7 T, liver ^{1}H MRS has only been applied using a relatively small surface coil for both transmit and receive.[12,22] Such a setup suffers from large B_1 inhomogeneities, and penetration depth is very limited. By using eight transmit-receive fractionated dipole antennas with 16 additional, integrated receive loops on a parallel transmit system and by applying RF phase shimming, we obtained high-quality images in which the whole liver anatomy was clearly visible (Figure 2A). This provided more freedom for and a better definition of the positioning of the MRS voxel (see Figure S1 of the supporting material for Dixon scans and voxel planning in all six subjects). For the MC-STEAM spectra, adding the signals from the 16 receive loops increased the SNR by a factor of 1.9 on average as compared with using the signals from the eight dipole antennas only (Figure S2 of the supporting material), which is in good correspondence with previous MRI data with this setup.[14]

In the previously reported study, Gajdošík et al presented an elegant approach to acquire ultrashort-T_E STEAM ^{1}H MR spectra in the liver at 7 T without water suppression, with switching of the spoiler gradients for sideband reduction.[12] The water resonance was removed from the lipid spectra during post-processing, which involved fitting of the water resonance by multiple Lorentzian lines which were subsequently subtracted from the spectra. During an MC measurement, the water signal is also retained, allowing for robust phase and frequency correction. Subtraction of downfield and upfield inverted spectra leads to a spectrum in which most of the water signal is canceled out and which is also free of gradient induced modulation sidebands. As such, MC presents an alternative method for non-water-suppressed liver ^{1}H MRS as compared with the

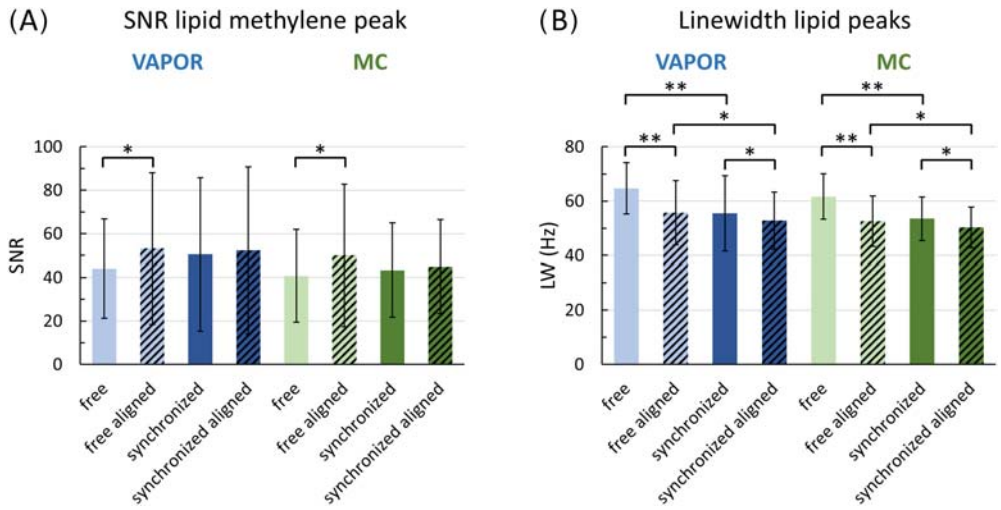

FIGURE 5 Average SNR for the lipid methylene peak (1.30 ppm) (A) and linewidth (LW) of the fitted lipid peaks (B) for the six subjects for both scan sessions from acquisitions with VAPOR-STEAM with free breathing (light blue) and synchronized breathing (dark blue), and MC-STEAM with free breathing (light green) and synchronized breathing (dark green). Results are shown for data reconstructed without (uniform colored bars) and with (colored bars with black hatches) frequency correction. For both SNR and LW, there was no significant difference between VAPOR and MC, but there was a significant interaction between the effects of reconstruction without and with frequency correction and measurements with free and synchronized breathing ($p = 0.04$ and $p = 0.03$ for SNR and LW, respectively). The significance signs in the figure represent the results of the Bonferroni corrected post-hoc tests for VAPOR and MC data taken together. $^{*}p < 0.05$, $^{**}p < 0.01$, both independent of measurement method (VAPOR or MC)

approach presented by Gajdošík et al. However, the in vivo MC-STEAM difference spectra did not resolve the olefinic lipid signal at 5.3 ppm, while this signal could readily be detected in most in vivo VAPOR-STEAM spectra. The culprit for this was the larger bandwidth of the frequency range untouched by the MC pulses of 350 Hz compared with the VAPOR water suppression bandwidth of 200 Hz for the in vivo measurements. We refrained from reducing the bandwidth of the non-inverted frequency range in the in vivo MC experiments, since it is important not to affect the water signal by the MC pulses, if the water signal is to be used for phase and frequency corrections and for quantification. In phantom measurements, reducing the bandwidth of the non-inverted frequency range from 350 Hz to 100 Hz resolved the olefinic lipid signal (Figure 1B,C), but also reduced the water signal amplitude by 13%. In the presence of frequency shifts due to motion, reducing the bandwidth of the non-inverted frequency range will likely lead to even greater reductions in water signal amplitude. Another reason not to shift the offsets for the MC pulses closer to the water frequency is that it would increase the required B_1^+ for full inversion of the lipid methylene peak (which was 15 μT for an offset of 175 Hz), which may not be achieved in all cases. Moreover, even though the olefinic lipid signal could be detected in most VAPOR-STEAM spectra, phantom measurements using the same water suppression bandwidth (200 Hz) as in the in vivo experiments showed that the olefinic peak amplitude was 23% lower and thus partially suppressed as compared with a VAPOR bandwidth of 100 Hz. Therefore, we decided not to use the olefinic lipid signal for quantification.

While the simultaneous acquisition of both water and metabolite signals is an advantage of MC, it also presents a limitation. When water and metabolite signals are acquired in separate acquisitions, the frequency offset is typically adjusted between the two scans to minimize the chemical shift displacement error (CSDE) between water and the metabolite of interest. With MC, this is not possible and the resulting CSDE between the voxel positioning for the water and lipid frequencies (Figure 2A) could therefore potentially compromise the quantification of the lipid signals with respect to the water signal. However, during voxel planning we took the CSDE into account and we assumed that the liver tissue composition across the area covering the voxels at the water and lipid methylene frequencies was homogeneous enough to allow for meaningful quantification of the results.

For the MC-STEAM acquisitions, the robust phase and frequency correction of individual acquisitions using the water signal resulted in spectra with similar SNR and linewidths for measurements with free breathing and measurements with synchronized breathing. The variability between liver lipid content determined from MC-STEAM spectra measured with free and synchronized breathing (CV = 8.3%) was in fact comparable to the intra-session variability with synchronized breathing (CV = 9.6%). The voxel that we used for the MRS measurements was rather small ($15 \times 15 \times 20$ mm^3) and was surrounded by homogeneous liver tissue. Therefore, even in the case of motion, the voxel was likely still within liver tissue. It should be noted though that the possibility of not quite homogenously distributed lipids and lipid compositions within the liver will influence the measurement uncertainty introduced by subject motion during the measurement. Obviously, in smaller and/or less homogeneous organs, motion could lead to inaccurate results and synchronized breathing or some sort of gating would be required. Nonetheless, the finding that, in the liver, MC-STEAM with free breathing performs equally well as MC-STEAM with synchronized breathing indicates that MC-STEAM does not

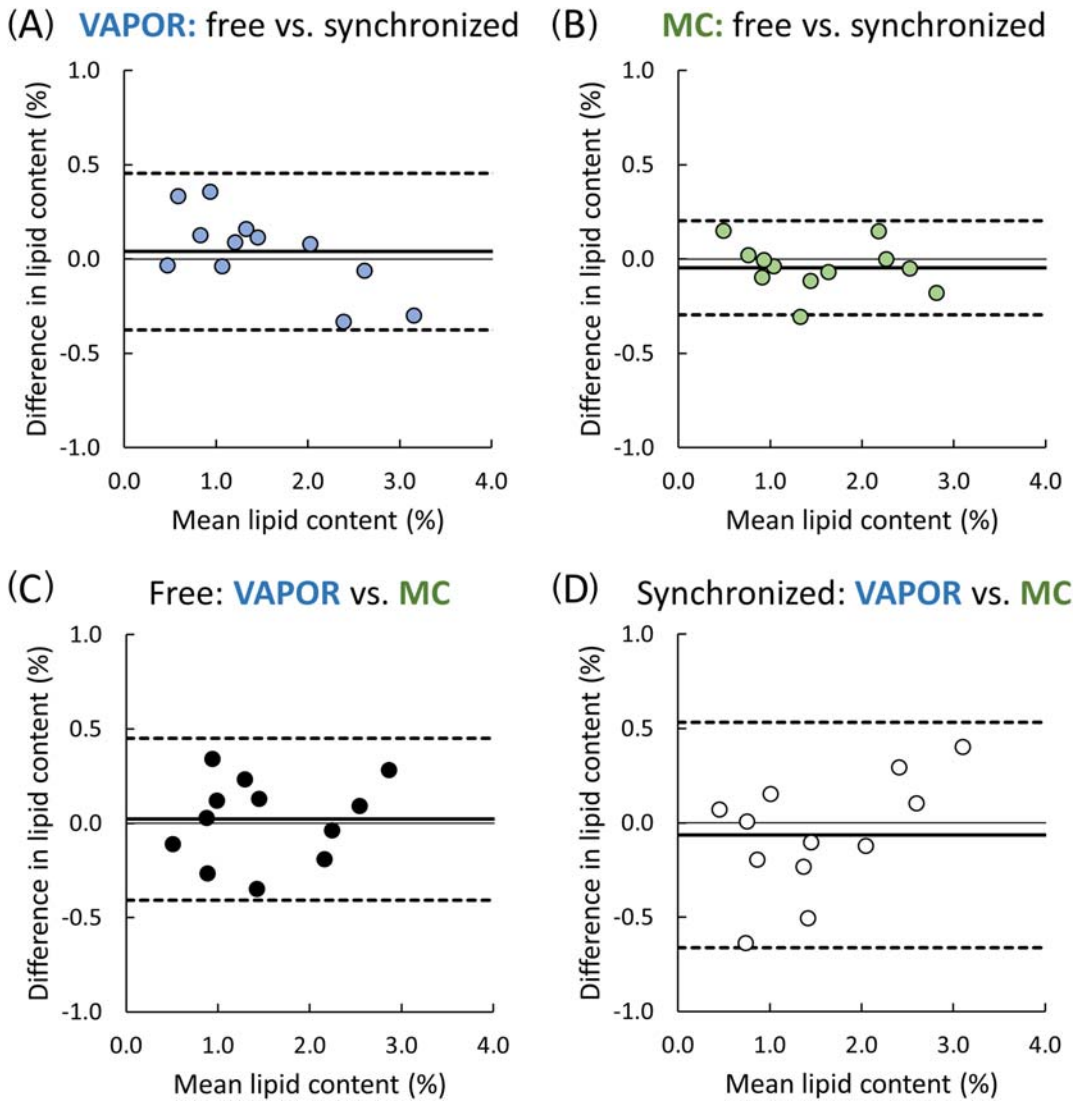

FIGURE 6 Bland-Altman plots for comparisons of liver lipid content between scans with free breathing and synchronized breathing acquired with VAPOR-STEAM (A) and MC-STEAM (B) and for comparisons between scans with VAPOR-STEAM and MC-STEAM obtained with free breathing (C) and synchronized breathing (D). Spectra were reconstructed with frequency correction. The solid black line shows the bias from zero (thin black line) and the dashed black lines mark ±1.96 SD. A, Absolute bias = 0.04%, CR = 0.42%, CV = 14.1%; B, absolute bias = 0.05%, CR = 0.25%, CV = 8.3%; C, absolute bias = 0.02%, CR = 0.45%, CV = 14.4%; D, absolute bias = 0.06%, CR = 0.60%, CV = 20.0%

require synchronization with respiratory motion, and that the robust phase and frequency correction enabled by MC is able to compensate for additional measurement uncertainties introduced by subject motion. Especially in clinical settings, where patients may struggle with holding their breath or breathing in a very controlled way throughout the rather lengthy MRS measurements, this is very useful. In the studies of Gajdošík et al, volunteers were placed on the surface coil in a right lateral position to minimize abdominal motion and instructed to breathe flatly and regularly.[12,22] While this approach proved to be feasible in a number of patient studies,[33,34] it may not be possible in all patients, as exemplified in another study, where some volunteers had to be scanned in a supine position because of space restrictions.[35] The use of a respiratory belt or navigator for real-time or retrospective respiratory gating is also not without problems (eg loss of signal from respiratory belt or low-quality navigator signal because of B_0 and B_1 inhomogeneities, especially at high field) and leads to increased scan times.[36]

For the VAPOR-STEAM spectra, the performance of the frequency correction was not optimal in 54% of the data sets for subjects with liver lipid contents lower than 2%, even though this was not directly apparent from the SNR and linewidth figures. The variability between liver lipid content measured with free and synchronized breathing was higher for VAPOR-STEAM (CV = 14.1%) than for MC-STEAM (CV = 8.3%). Also, the intra-session variability for liver lipid content quantification with VAPOR-STEAM with synchronized breathing (CV = 12.2%) was slightly higher than for MC-STEAM with synchronized breathing (CV = 9.6%) and the intra-session variability of UI was much larger for VAPOR-STEAM (CV = 51.7%) than for MC-STEAM (CV = 17.2%). These higher variabilities could likely be explained by less robust phase and frequency

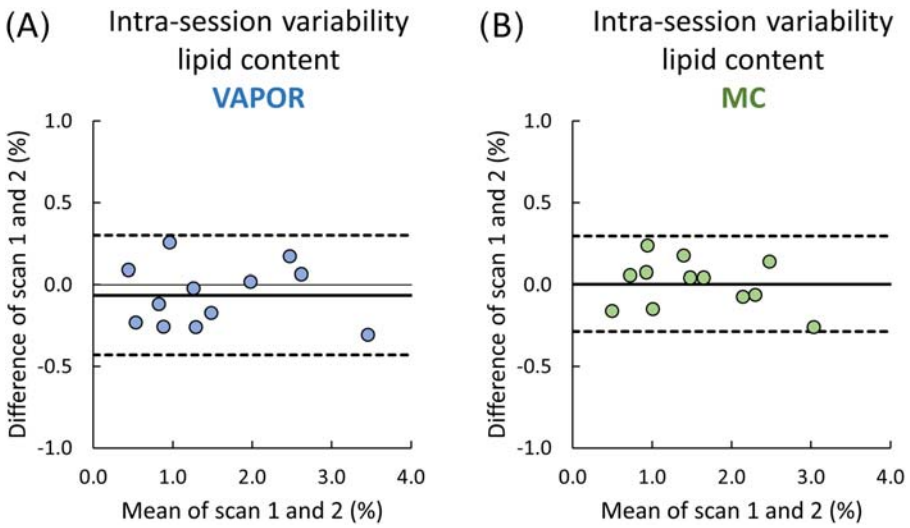

FIGURE 7 Bland-Altman plots of intra-session variability in liver lipid content measured with VAPOR-STEAM (A) and MC-STEAM (B) with synchronized breathing. Spectra were reconstructed with frequency correction. The solid black line shows the bias from zero (thin black line) and the dashed black lines mark ±1.96 SD. A, Absolute bias = 0.06%, CR = 0.36%, CV = 12.2%; B, absolute bias = 0.00%, CR = 0.29%, CV = 9.6%

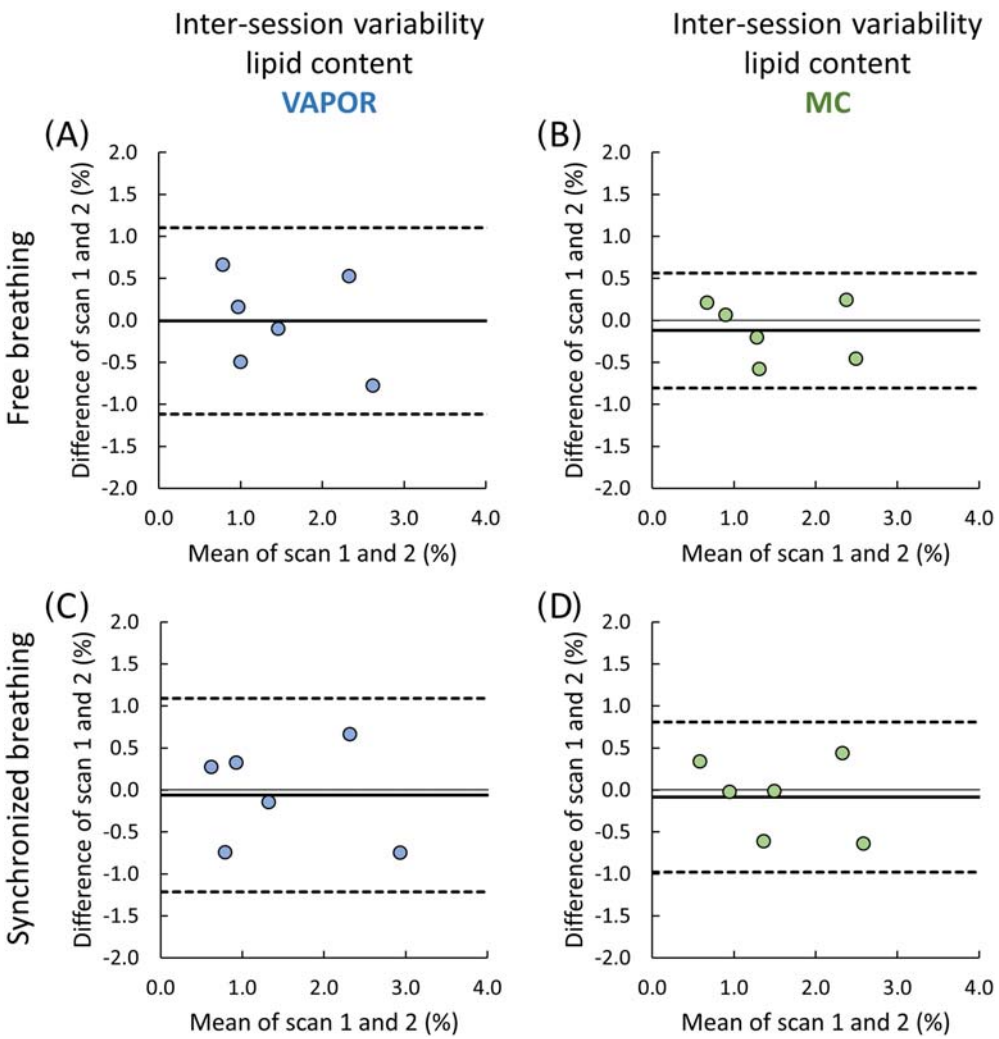

FIGURE 8 Bland-Altman plots of inter-session variability in liver lipid content measured with VAPOR-STEAM (A, C) and MC-STEAM (B, D) with free breathing (A, B) and synchronized breathing (C, D). Spectra were reconstructed with frequency correction. The solid black line shows the bias from zero (thin black line) and the dashed black lines mark ±1.96 SD. A, Absolute bias = 0.01%, CR = 1.11%, CV = 37.1%; B, absolute bias = 0.12%, CR = 0.68%, CV = 23.2%; C, absolute bias = 0.06%, CR = 1.15%, CV = 39.5%; D, absolute bias = 0.09%, CR = 0.90%, CV = 29.4%

corrections in the case of VAPOR-STEAM, due to the low SNR of the lipid signals in the individual acquisitions. However, liver lipid content as determined by VAPOR-STEAM and MC-STEAM over all measurements did not significantly differ.

The inter-session variability of liver lipid content quantification was better for MC-STEAM (CV = 23.2% and 29.4% for free and synchronized breathing, respectively) than for VAPOR-STEAM (CV = 37.1% and 39.5% for free and synchronized breathing, respectively), but was relatively

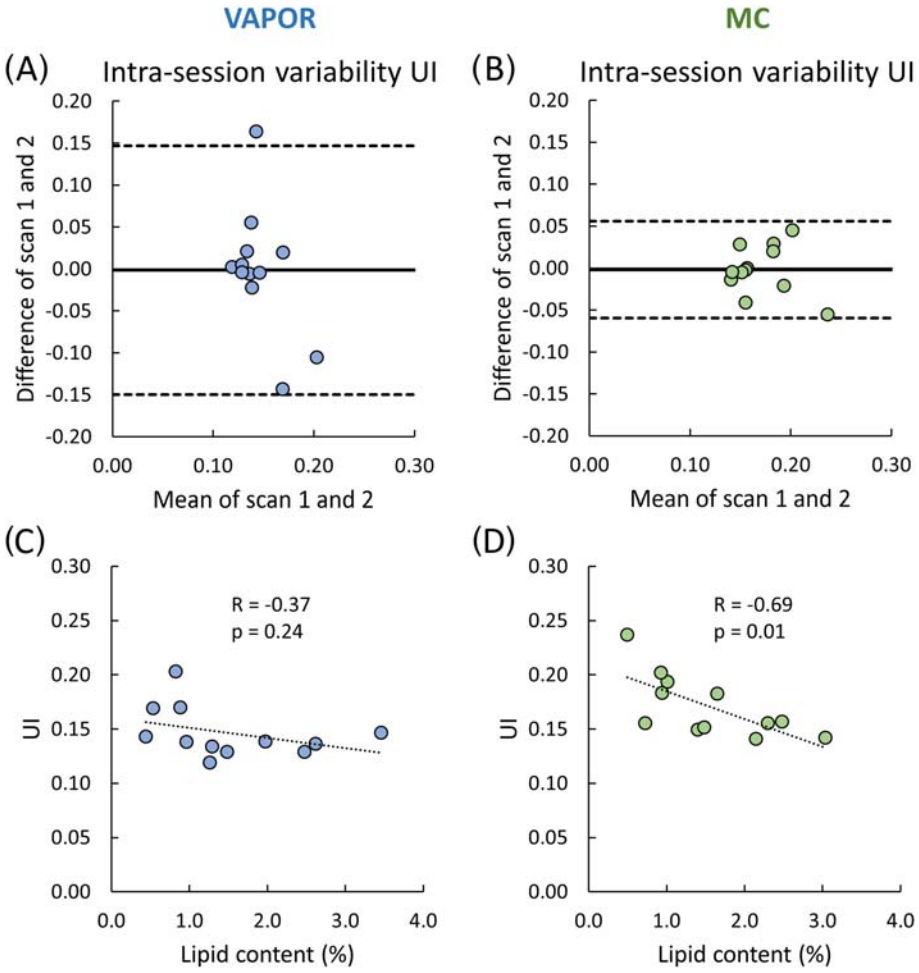

FIGURE 9 A, B, Bland-Altman plots of intra-session variability in UI of hepatic lipids measured with VAPOR-STEAM (A) and MC-STEAM (B) with synchronized breathing. Spectra were reconstructed with frequency correction. The solid black line shows the bias from zero (thin black line) and the dashed black lines mark ±1.96 SD. A, Absolute bias = 0.00, CR = 0.15, CV = 51.7%; B, absolute bias = 0.00, CR = 0.06, CV = 17.2%. C, D, UI versus liver lipid content for the six subjects for both scan sessions. Data were measured with VAPOR-STEAM (C) and MC-STEAM (D) with synchronized breathing, and results of the two measurements acquired during one session were averaged. With MC-STEAM a significant negative correlation was observed, while the data acquired with VAPOR-STEAM did not indicate a clear relationship

poor as compared with previous studies (CV < 10%).[7,10,12,37,38] However, in most of those studies[7,10,12,37] variability was determined on the same day, and all of them included obese subjects with fatty livers. In the present study, subjects were scanned twice on two separate days, approximately one week apart, and all subjects had liver lipid contents lower than 4%. Therefore small absolute differences can already result in large relative differences, and part of the inter-session variability in the current study may also be explained by real, biological differences in liver lipid content between the two sessions, because conditions such as nutrition and physical activity were not standardized. This is corroborated by a previous study showing that the variability of liver lipid content over one month was significantly greater than the within-day reproducibility (CV = 44% versus 7% in subjects without diabetes).[39] Moreover, it has been demonstrated that both diet and exercise affect liver lipid content.[40,41]

The UI of hepatic lipids, as determined from the MC-STEAM measurements, was found to be negatively correlated with liver lipid content, even though the liver lipid contents of our subjects all fall in a very narrow range. This is in agreement with previous findings that UI decreases with liver lipid content in NAFLD patients[5,42] and in healthy subjects with a broad range of liver lipid contents,[12] and extends the relationship also to the regime of very low liver lipid contents.

In conclusion, non-water-suppressed MC-STEAM on a 7 T system with parallel transmit is a promising approach for ^{1}H MRS applications in the body that are affected by motion, such as in the liver. Robust phase and frequency correction of individual acquisitions before averaging, enabled by the preserved water signal in MC-STEAM, yields better repeatability and reproducibility compared with water-suppressed measurements.

ACKNOWLEDGEMENTS

We thank Katharina S. Milde for her contributions to the liver ^{1}H MRS protocol and data reconstruction and processing pipeline. This work was supported by a travel grant to AF from the Nederlandse Organisatie voor Wetenschappelijk Onderzoek (NWO) (project 040.11.634) and by funding from the Millennium Science Initiative of the Ministry of Economy, Development and Tourism, Chile (grant Nucleus for Cardiovascular Magnetic Resonance). Furthermore, the following grants are acknowledged: CONICYT-PCHA/Doctorado Nacional (2016-21160835) and FONDECYT (1180525).

ORCID

Jeanine J. Prompers https://orcid.org/0000-0002-4756-4474

REFERENCES

1. Angulo P. Nonalcoholic fatty liver disease. *N Engl J Med*. 2002;346(16):1221-1231.
2. Cohen JC, Horton JD, Hobbs HH. Human fatty liver disease: old questions and new insights. *Science*. 2011;332(6037):1519-1523.
3. Araya J, Rodrigo R, Videla LA, et al. Increase in long-chain polyunsaturated fatty acid $n-6/n-3$ ratio in relation to hepatic steatosis in patients with non-alcoholic fatty liver disease. *Clin Sci*. 2004;106(6):635-643.
4. Elizondo A, Araya J, Rodrigo R, et al. Polyunsaturated fatty acid pattern in liver and erythrocyte phospholipids from obese patients. *Obesity*. 2007;15(1):24-31.
5. Puri P, Baillie RA, Wiest MM, et al. A lipidomic analysis of nonalcoholic fatty liver disease. *Hepatology*. 2007;46(4):1081-1090.
6. Hamilton G, Yokoo T, Bydder M, et al. In vivo characterization of the liver fat ^{1}H MR spectrum. *NMR Biomed*. 2011;24(7):784-790.
7. Johnson NA, Walton DW, Sachinwalla T, et al. Noninvasive assessment of hepatic lipid composition: advancing understanding and management of fatty liver disorders. *Hepatology*. 2008;47(5):1513-1523.
8. Longo R, Pollesello P, Ricci C, et al. Proton MR spectroscopy in quantitative in vivo determination of fat content in human liver steatosis. *J Magn Reson Imaging*. 1995;5(3):281-285.
9. Reeder SB, Cruite I, Hamilton G, Sirlin CB. Quantitative assessment of liver fat with magnetic resonance imaging and spectroscopy. *J Magn Reson Imaging*. 2011;34(4):729-749.
10. Szczepaniak LS, Nurenberg P, Leonard D, et al. Magnetic resonance spectroscopy to measure hepatic triglyceride content: prevalence of hepatic steatosis in the general population. *Am J Physiol Endocrinol Metab*. 2005;288(2):E462-E468.
11. Lundbom J, Hakkarainen A, Soderlund S, Westerbacka J, Lundbom N, Taskinen MR. Long-TE ^{1}H MRS suggests that liver fat is more saturated than subcutaneous and visceral fat. *NMR Biomed*. 2011;24(3):238-245.
12. Gajdošík M, Chadzynski GL, Hangel G, et al. Ultrashort-TE stimulated echo acquisition mode (STEAM) improves the quantification of lipids and fatty acid chain unsaturation in the human liver at 7 T. *NMR Biomed*. 2015;28(10):1283-1293.
13. Raaijmakers AJ, Italiaander M, Voogt IJ, et al. The fractionated dipole antenna: a new antenna for body imaging at 7 Tesla. *Magn Reson Med*. 2016;75(3):1366-1374.
14. Steensma BR, Voogt IJ, Leiner T, et al. An 8-channel Tx/Rx dipole array combined with 16 Rx loops for high-resolution functional cardiac imaging at 7 T. *Magn Reson Mater Phys Biol Med*. 2018;31(1):7-18.
15. Dreher W, Leibfritz D. New method for the simultaneous detection of metabolites and water in localized in vivo ^{1}H nuclear magnetic resonance spectroscopy. *Magn Reson Med*. 2005;54(1):190-195.
16. de Graaf RA, Sacolick LI, Rothman D. Water and metabolite-modulated MR spectroscopy and spectroscopic imaging. *Proc Int Soc Magn Reson Med*. 2006;14:3063.
17. MacMillan EL, Chong DG, Dreher W, Henning A, Boesch C, Kreis R. Magnetization exchange with water and T_1 relaxation of the downfield resonances in human brain spectra at 3.0 T. *Magn Reson Med*. 2011;65(5):1239-1246.
18. Fillmer A, Hock A, Cameron D, Henning A. Non-water-suppressed ^{1}H MR spectroscopy with orientational prior knowledge shows potential for separating intra- and extramyocellular lipid signals in human myocardium. *Sci Rep*. 2017;7(1):16898.
19. Giapitzakis IA, Shao T, Avdievich N, Mekle R, Kreis R, Henning A. Metabolite-cycled STEAM and semi-LASER localization for MR spectroscopy of the human brain at 9.4T. *Magn Reson Med*. 2018;79(4):1841-1850.
20. Hock A, MacMillan EL, Fuchs A, et al. Non-water-suppressed proton MR spectroscopy improves spectral quality in the human spinal cord. *Magn Reson Med*. 2013;69(5):1253-1260.
21. Hwang TL, van Zijl PC, Garwood M. Asymmetric adiabatic pulses for NH selection. *J Magn Reson*. 1999;138(1):173-177.
22. Gajdošík M, Chmelik M, Just-Kukurova I, et al. In vivo relaxation behavior of liver compounds at 7 Tesla, measured by single-voxel proton MR spectroscopy. *J Magn Reson Imaging*. 2014;40(6):1365-1374.
23. Tkac I, Starcuk Z, Choi IY, Gruetter R. In vivo ^{1}H NMR spectroscopy of rat brain at 1 ms echo time. *Magn Reson Med*. 1999;41(4):649-656.
24. Metzger GJ, Snyder C, Akgun C, Vaughan T, Ugurbil K, Van de Moortele PF. Local B_1^+ shimming for prostate imaging with transceiver arrays at 7T based on subject-dependent transmit phase measurements. *Magn Reson Med*. 2008;59(2):396-409.
25. Yarnykh VL. Actual flip-angle imaging in the pulsed steady state: a method for rapid three-dimensional mapping of the transmitted radiofrequency field. *Magn Reson Med*. 2007;57(1):192-200.
26. Fillmer A, Kirchner T, Cameron D, Henning A. Constrained image-based B_0 shimming accounting for "local minimum traps" in the optimization and field inhomogeneities outside the region of interest. *Magn Reson Med*. 2015;73(4):1370-1380.
27. Dixon WT. Simple proton spectroscopic imaging. *Radiology*. 1984;153(1):189-194.
28. An L, Willem van der Veen J, Li S, Thomasson DM, Shen J. Combination of multichannel single-voxel MRS signals using generalized least squares. *J Magn Reson Imaging*. 2013;37(6):1445-1450.
29. Roemer PB, Edelstein WA, Hayes CE, Souza SP, Mueller OM. The NMR phased array. *Magn Reson Med*. 1990;16(2):192-225.
30. Wiegers EC, Philips BWJ, Heerschap A, van der Graaf M. Automatic frequency and phase alignment of in vivo J-difference-edited MR spectra by frequency domain correlation. *Magn Reson Mater Phys Biol Med*. 2017;30(6):537-544.
31. Stefan D, Di Cesare F, Andrasescu A, et al. Quantitation of magnetic resonance spectroscopy signals: the jMRUI software package. *Meas Sci Technol*. 2009;20(10):104035.
32. Vanhamme L, van den Boogaart A, Van Huffel S. Improved method for accurate and efficient quantification of MRS data with use of prior knowledge. *J Magn Reson*. 1997;129(1):35-43.
33. Wolf P, Fellinger P, Pfleger L, et al. Reduced hepatocellular lipid accumulation and energy metabolism in patients with long standing type 1 diabetes mellitus. *Sci Rep*. 2019;9(1):2576.
34. Smajis S, Gajdošík M, Pfleger L, et al. Metabolic effects of a prolonged, very-high-dose dietary fructose challenge in healthy subjects. *Am J Clin Nutr*. 2020;111(2):369-377.

35. Fellinger P, Wolf P, Pfleger L, et al. Increased ATP synthesis might counteract hepatic lipid accumulation in acromegaly. *JCI Insight*. 2020;5(5):e134638.
36. Peereboom SM, Gastl M, Fuetterer M, Kozerke S. Navigator-free metabolite-cycled proton spectroscopy of the heart. *Magn Reson Med*. 2020;83(3):795-805.
37. Thomas EL, Hamilton G, Patel N, et al. Hepatic triglyceride content and its relation to body adiposity: a magnetic resonance imaging and proton magnetic resonance spectroscopy study. *Gut*. 2005;54(1):122-127.
38. van Werven JR, Hoogduin JM, Nederveen AJ, et al. Reproducibility of 3.0 Tesla magnetic resonance spectroscopy for measuring hepatic fat content. *J Magn Reson Imaging*. 2009;30(2):444-448.
39. Stephenson MC, Leverton E, Khoo EY, et al. Variability in fasting lipid and glycogen contents in hepatic and skeletal muscle tissue in subjects with and without type 2 diabetes: a ^{1}H and ^{13}C MRS study. *NMR Biomed*. 2013;26(11):1518-1526.
40. Cheng S, Ge J, Zhao C, et al. Effect of aerobic exercise and diet on liver fat in pre-diabetic patients with non-alcoholic-fatty-liver-disease: a randomized controlled trial. *Sci Rep*. 2017;7(1):15952.
41. Shah K, Stufflebam A, Hilton TN, Sinacore DR, Klein S, Villareal DT. Diet and exercise interventions reduce intrahepatic fat content and improve insulin sensitivity in obese older adults. *Obesity*. 2009;17(12):2162-2168.
42. Hamilton G, Schlein AN, Wolfson T, et al. The relationship between liver triglyceride composition and proton density fat fraction as assessed by ^{1}H MRS. *NMR Biomed*. 2020;33(6):e4286.

SUPPORTING INFORMATION

Additional supporting information may be found online in the Supporting Information section at the end of this article.

How to cite this article: Xavier A, Arteaga de Castro C, Andia ME, et al. Metabolite cycled liver ^{1}H MRS on a 7 T parallel transmit system. *NMR in Biomedicine*. 2020;33:e4343. https://doi.org/10.1002/nbm.4343